ACS APPLIED MATERIALS & INTERFACES

Letter

www.acsami.org

Synergistic Effects of Doping and Thermal Treatment on Organic Semiconducting Nanowires

Sung-Yong Min, Young-Hoon Kim, Christoph Wolf, and Tae-Woo Lee*

Department of Materials Science and Engineering, Pohang University of Science and Technology (POSTECH), Pohang 790−784, Republic of Korea

Supporting Information

ABSTRACT: Doping of small molecular donors or acceptors on conjugated organic materials can be used to improve the performance of organic electronics. Here we demonstrate highly aligned poly(3-hexylthiophene) (P3HT) nanowires (NWs) doped with 2,3,5,6-tetrafluoro-7,7,8,8-tetracyanoquinodimethane (F4-TCNQ) using electrohydrodynamic organic NW printing. The transistor based on *p*-doped NWs had an order of magnitude higher mobility than did the undoped NW device. This significant improvement resulted from the synergistic effects of *p*-type doping and thermal annealing on F4-TCNQ-doped P3HT NWs, which induce microstructure changes in P3HT chains.

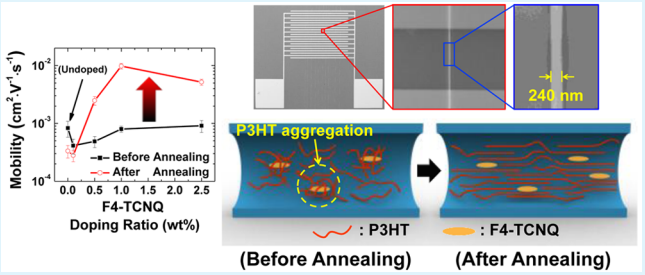

KEYWORDS: *electrohydrodynamic organic nanowire printing, p-type dopant, thermal annealing, organic field-effect transistors, polymer microstructure*

One-dimensional organic semiconducting nanowires (OSNWs) have excellent physical properties and potential as building blocks for highly integrated nanoelectronics including transistors, light-emitting devices, energy harvesting devices, and sensors.[1−7] Until now, practical device applications of OSNWs have been limited because of the lack of reliable technique for individual control of nanowires (NWs). Our previous reports suggested the possibility of large-scale alignment and device applications of OSNWs using electrohydrodynamic organic nanowire printing (ONP) technique.[8−12] Printing and alignment of poly(3-hexylthiophene) (P3HT) NWs and electronics applications including field-effect transistors (FETs) and complementary inverters were successfully demonstrated. ONP can be a promising strategy for applications in the field of organic nanoelectronics.

Until now, the aligned or unaligned polymer nanowires showed low charge carrier mobility (~1 × 10^{-3} cm^2 V^{-1} s^{-1}). To enhance the carrier mobility of organic materials, there have been several strategies including synthesis of new small moleucules and polymers,[13−16] surface modification,[17,18] thermal annealing[19] and molecular doping.[20−24] Among them, molecular doping approach using small molecular donors or acceptors in conjugated organic materials is an effective way to enhance the characteristics of organic FETs. Strong electron acceptors can significantly enhance the bulk conductivity and hole current of conjugated polymers and effectiveness of *p*-doping increased in shallower highest occupied molecular orbital (HOMO) level of the polymers.[22] *p*-Doping and thermal annealing can increase the crystalline ordering and electrical characteristics in P3HT films.[23,25] However, these approaches are only applicable to the thin film geometry, which can easily form ordered domains during spin-casting process and improve the crystalline ordering after thermal annealing because of unconstrained polymer chain movement. In contrast, it is hard to form ordered domains in NW geometry with constrained dimension; in our previous report, printed P3HT NWs showed extended chain morphology along the wire axis, not the lamella structure.[8] Furthermore, collecting densely aligned NWs enough to analyze the chain morphology has been a tough issue. For these limitations, there were no studies on investigating the effect of molecular doping and thermal annealing to chain morphology and electrical characteristics of OSNWs along the wire axis.

Here we report enhanced charge transport characteristics in highly aligned P3HT NW FETs using two strategies: (i) *p*-type doping and (ii) thermal annealing. 2,3,5,6-Tetrafluoro-7,7,8,8-tetracyanoquinodimethane (F4-TCNQ) was used as a *p*-type dopant because of its strong electron affinity (lowest unoccupied molecular orbital: 5.2 eV).[22] When the *p*-type semiconducting polymer, P3HT, was doped with the F4-TCNQ, the charge carrier density in the P3HT increased due to charge transfer from P3HT to F4-TCNQ. Thermal annealing is an important process to activate the doping effect. It induces change of microstructure of P3HT chains and enhanced charge transport characteristics. Furthermore, unlike conventional OSNWs preparation methods, highly aligned P3HT NWs were prepared using the ONP technique. Then we analyzed the synergistic effect of doping and thermal annealing

Received: July 7, 2015
Accepted: August 18, 2015
Published: August 18, 2015

DOI: 10.1021/acsami.5b05647
ACS Appl. Mater. Interfaces 2015, 7, 18909−18914

on the microstructure of P3HT chains using polarized spectroscopy along the wire axis.

Figure 1a shows the schematic representation of ONP process. The ONP system consists of a movable motorized

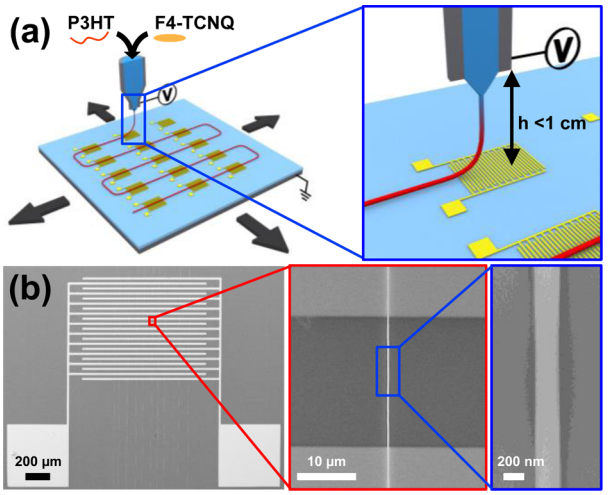

Figure 1. Aligned F4-TCNQ doped P3HT NW FET. (a) Schematic representation of organic nanowire printing process. (b) Scanning electron microscope images of highly aligned F4-TCNQ-doped P3HT NW FET.

stage and a delivery nozzle mounted above it. By moving the nozzle tip containing a polymer solution within 1 cm of a flat ground collector and applying a high voltage of 1.5−2 kV, p-doped P3HT NWs can be printed and aligned with desired position and orientation.

The basic architecture of the device consists of a Si/SiO_2 (100 nm) substrate, Ti (3 nm)/Au (30 nm) for source and drain electrodes with interdigitated structure, and P3HT NWs. First, the electrodes were deposited on the substrate, then highly aligned *p*-doped P3HT NWs were fabricated with 0.1, 0.5, 1, 2 wt % ratios of F4-TCNQ to P3HT. Ten strands of highly aligned F4-TCNQ doped P3HT NWs with an average diameter of 274.1 ± 36.7 nm were successfully printed on the device substrate (Figure 1b).

The FETs of undoped and F4-TCNQ doped P3HT NWs showed typical behaviors of *p*-type organic FETs (Figure 2; Figure S1). As the doping ratio of F4-TCNQ increased, maximum on-current level and field-effect mobility (μ_{FET}) of FETs increased (Figure 2a). The current increase occurred because the number of charge carriers increases with the concentration of F4-TCNQ.[26] However, the improvement of performance parameters by doping was not obvious before thermal annealing. Before annealing, general characteristics of doped P3HT NW FETs were lower than that of undoped P3HT NW device. The electrical characteristics of doped P3HT NW FETs were remarkably increased after annealing (Figure 2b). After thermal annealing at 200 °C, the on-current level and the μ_{FET} were surprisingly increased more than an order of magnitude (maximum μ_{FET} = 9.78 × 10^{-3} cm^2 V^{-1} s^{-1}) compared with those before annealing (Table 1). These results were also consistent with the annealing temperature dependency of electrical characteristics in doped NW FETs (Figure 3 and Table 2). As the annealing temperature increased with 100, 150, 200 °C in the 1 wt % F4-TCNQ doped P3HT NW FETs, the maximum on-current level and the μ_{FET} of doped NW FETs increased.

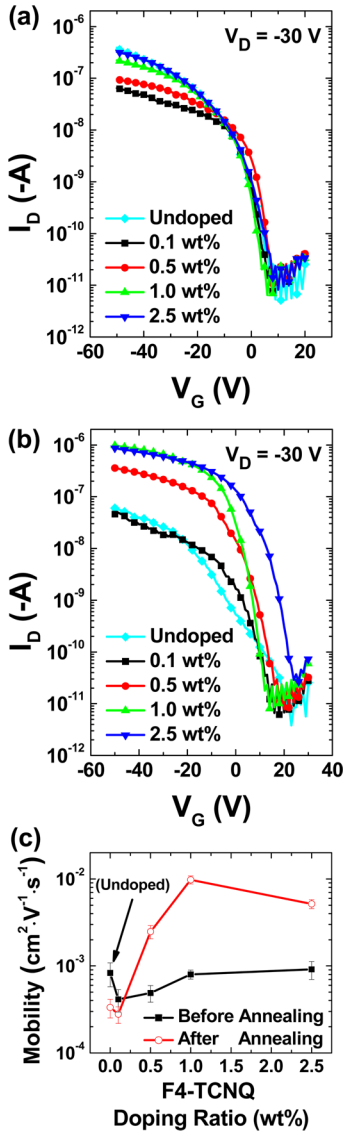

Figure 2. Transfer characteristics ($I_D - V_G$) of P3HT NW FET doped with various concentrations of F4-TCNQ (a) before and (b) after thermal annealing at 200 °C for 1 h. (c) μ_{FET} of F4-TCNQ doped P3HT NW FETs before (close square) and after (open circle) annealing.

The origin of the electrical characteristics enhancement is not related with either thermal annealing or F4-TCNQ doping separately, because the electrical performance of (i) undoped/annealed and (ii) doped/unannealed NW FETs were degraded than that of pristine (undoped/unannealed) NW FETs (Figure 2). The former (undoped/annealed NW) might be influenced by poly(ethylene oxide) (PEO) which was added to increase the viscosity of printing solution, because the PEO shell directly contacting the underlying gate dielectric can be diffused into the P3HT core during thermal annealing and the diffused PEO can scatter charge transport of the channel in a bottom-gate device structure (Figure S2),[8] unlike our previous report in which we used a top-gate device structure:[9] PEO dewetted on P3HT did not affect the charge transport significantly. However, the doped NW FETs showed significantly increased μ_{FET} after thermal annealing. It suggests that thermal annealing can activate the doping effect of F4-TCNQ in P3HT NWs. The thermal activation of doping effect on F4-TCNQ doped NWs

DOI: 10.1021/acsami.5b05647
ACS Appl. Mater. Interfaces 2015, 7, 18909−18914

Table 1. Device Characteristics of F4-TCNQ-Doped P3HT NW FETs with Various Doping Ratios

	before annealing			after annealing		
doping ratio (wt %)	mobility ($cm^2\ V^{-1}\ s^{-1}$)	$I_{on/off}$	V_{th} (V)	mobility ($cm^2\ V^{-1}\ s^{-1}$)	$I_{on/off}$	V_{th} (V)
undoped	8.31×10^{-4}	5.50×10^{4}	1.86	3.34×10^{-4}	2.76×10^{4}	3.29
0.1	4.14×10^{-4}	9.81×10^{3}	3.15	2.80×10^{-4}	4.45×10^{3}	13.11
0.5	4.89×10^{-4}	1.09×10^{4}	4.41	2.49×10^{-3}	5.35×10^{4}	14.55
1	8.00×10^{-4}	2.48×10^{4}	3.30	9.78×10^{-3}	1.28×10^{5}	14.83
2.5	9.11×10^{-4}	3.01×10^{4}	3.87	5.17×10^{-3}	3.40×10^{4}	18.34

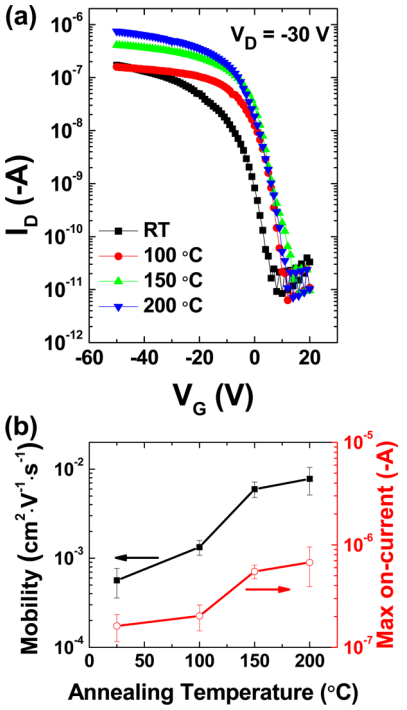

Figure 3. (a) Transfer characteristics ($I_D - V_G$) of F4-TCNQ doped (1 wt %) P3HT NW FET with various annealing temperatures. (b) μ_{FET} (close square) and maximum on-currents (open circle) of F4-TCNQ-doped P3HT NW FETs with different annealing temperatures.

Table 2. Device Characteristics of F4-TCNQ-Doped P3HT NW FETs with Various Annealing Conditions

annealing temperature (°C)	mobility ($cm^2\ V^{-1}\ s^{-1}$)	$I_{on/off}$	V_{th} (V)
RT	5.64×10^{-4}	1.24×10^{4}	3.30
100	1.33×10^{-3}	1.96×10^{4}	12.17
150	5.97×10^{-3}	8.98×10^{4}	13.18
200	7.79×10^{-3}	1.12×10^{5}	14.83

resulted in better charge transfer interactions between P3HT chains and F4-TCNQ molecules[26,27] and better hole transport in NWs. The reduced photoluminescence (PL) lifetime in 1 wt % *p*-doped P3HT NWs (0.43 ns) compared with undoped NWs (0.60 ns) supports the formation of charge transfer complexes between P3HT and F4-TCNQ (Figure S3).[22] The diffused PEO into the P3HT core may also interrupt the charge transport in doped NW after thermal annealing; however, enhancement by the doping was more dominant than degradation by the PEO diffusion with the doping ratios >0.5 wt %.

It is notable that threshold voltages (V_{th}) of devices shifts with increased doping ratios and annealing temperatures (Figure S4 and Tables 1 and 2). The V_{th} is related to the gate voltage where the number of charge carriers are equal to the number of surface trap states.[28] The number of mobile holes increases as a result of charge transfer complexes formation between P3HT and F4-TCNQ, which fills traps states and decreases the number, so it causes the shifts of V_{th} and μ_{FET}.[23] V_{th} shift is more significant in the devices after annealing than in the devices before annealing and with the higher annealing temperatures, which also supports the thermal activation of doping effect.

To verify the thermal activation of doping effect on F4-TCNQ-doped NWs, we performed polarized PL and UV−vis absorption spectroscopy analyses. The aligned NWs were oriented perpendicular to the ground (V position), and two polarizers in front of the exciting source light and detector were rotated in vertical (V) and horizontal (H) directions. Doped NWs both before and after annealing showed higher peak intensity when the exciting light and detection were polarized parallel to the wire axis (VVV) than when they were polarized in other directions (Figure 4a and b), which indicate that the backbone of P3HT was extended due to the strong electric field during the printing process; these results are consistent with the previously reported results.[8] To investigate the microstructure of P3HT NWs after doping and thermal annealing, we calculated fluorescence anisotropy (r) of each NWs from the results of polarized PL spectra as[29]

$$r = \frac{I_{VVV} - GI_{VVH}}{I_{VVV} + 2GI_{VVH}} \quad (1)$$

$$G = \frac{I_{VHV}}{I_{VHH}} \quad (2)$$

where I_{VVV} is the polarized PL intensity of when exciting light and detection polarizers are oriented parallel to the wire axis, I_{VVH} is the polarized PL intensity of when exciting light polarizer is oriented parallel to the wire axis, and detection polarizer is oriented perpendicular to the wire axis, I_{VHV} is the polarized PL intensity of when exciting light polarizer is oriented perpendicular to the wire axis, and detection polarizer is oriented parallel to the wire axis, and I_{VHH} is the polarized PL intensity of when exciting light and detection polarizers are oriented perpendicular to the wire axis.

The undoped/unannealed NWs had $r \approx 0.4$ (Figure 4c and refer to ref 8), which means that absorption dipoles and emission dipoles are colinear, and the degree of chain alignment along the wire axis is high.[29] The doped NWs showed decreased r to nearly zero, which indicates that emission dipoles are randomly oriented. The randomly oriented emission dipoles can be caused by aggregation of P3HT chains due to strong charge-transfer interaction between F4-TCNQ and P3HT, which is consistent with previous reports.[25,27] This random orientation results in low charge transport characteristics in the F4-TCNQ doped NW FETs. After thermal

DOI: 10.1021/acsami.5b05647
ACS Appl. Mater. Interfaces 2015, 7, 18909−18914

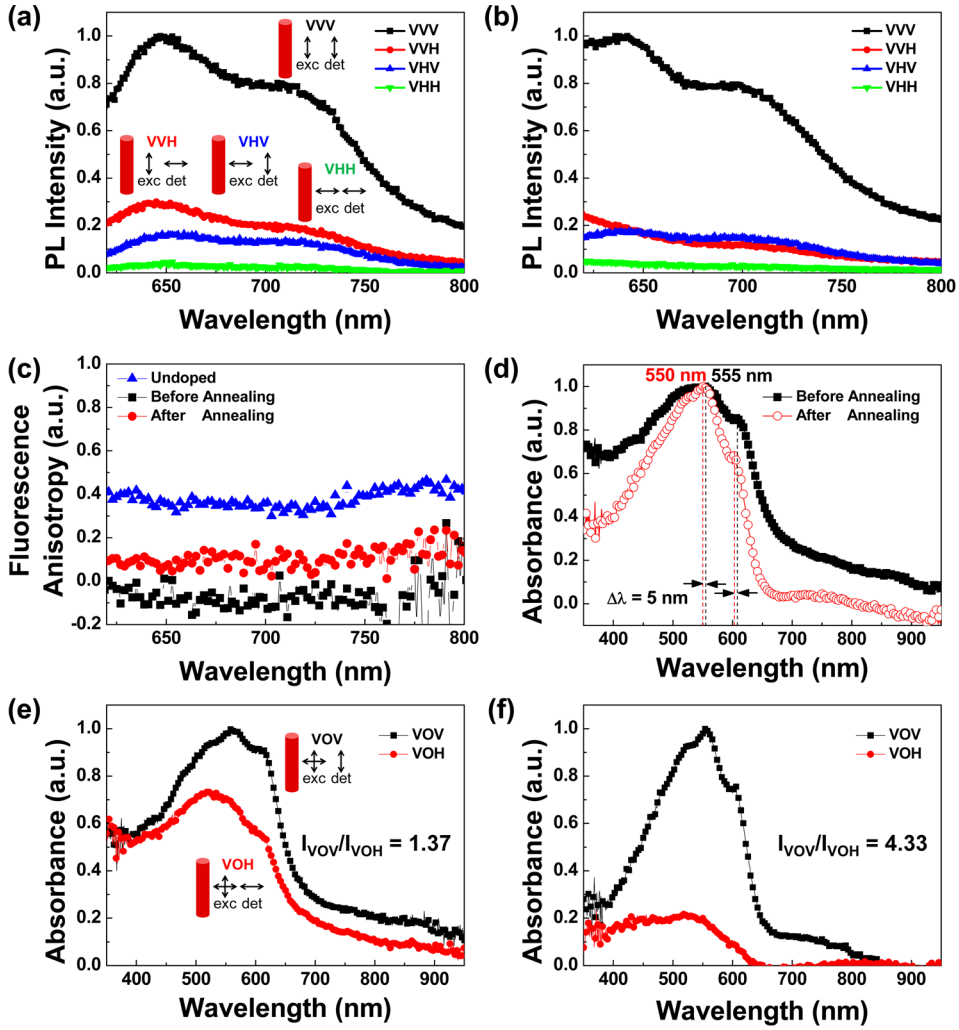

Figure 4. Polarized photoluminescence (PL) spectra of F4-TCNQ doped P3HT NWs (a) before and (b) after annealing (200 °C) with different polarization directions: (i) exciting light and detection polarized parallel to the wire axis (VVV), (ii) exciting light polarized perpendicular to the wire axis, and detection polarized parallel to the wire axis (VHV), (iii) exciting light polarized parallel to the wire axis, and detection polarized perpendicular to the wire axis (VVH), and (iv) exciting light and detection polarized perpendicular to the wire axis (VHH). (c) Fluorescence anisotropy of undoped and F4-TCNQ-doped P3HT NWs. (d) UV−vis absorption spectra of F4-TCNQ-doped P3HT NWs. Polarized UV−vis absorption spectra of F4-TCNQ-doped P3HT NWs (e) before and (f) after annealing with unpolarized exciting light; detection is polarized parallel (VOV) and perpendicular (VOH) to the wire axis.

annealing, r was increased compared with the doped/unannealed NWs because the electrostatic interaction between F4-TCNQ and P3HT chains was weakened by thermal movement, and because the aggregated P3HT chains were extended. Therefore, the enhanced electrical characteristics of F4-TCNQ doped NW FET after annealing results from the extended P3HT chain orientation and charge transfer between P3HT and F4-TCNQ molecules.

This result was confirmed using polarized UV−vis absorption spectroscopy. As the P3HT NWs were doped, their UV−vis absorption spectra were blue-shifted in comparison to the spectrum of undoped NWs (Figure 4d and refer to ref 8), which is associated with the aggregation of P3HT chains due to the strong interaction between P3HT and F4-TCNQ molecules.[25,30] After thermal annealing, intensity of shoulder at about 600 nm decreased compared with before annealing, which is related to decreased crystallinity and extended chains of P3HT.[8] Despite the lower crystallinity, charge transport in the NW FETs can be enhanced because the P3HT chains are extended along the wire axis. In polarized UV−vis absorption spectra, peak intensity ratio (I_{VOV}/I_{VOH}) was increased from 1.37 to 4.33 by thermal annealing of NWs (Figure 4e, f); this indicates an increase in absorption dipole anisotropy and confirms the results of fluorescence anisotropy change in the polarized PL spectra.

Finally, we can summarize the synergistic effect of p-type doping and thermal annealing on F4-TCNQ-doped P3HT NW in a schematic illustration (Figure 5): The thermal activation of F4-TCNQ doping effect is correlated with the microstructure of P3HT chains in the NWs. In undoped NWs, P3HT chains are extended along the wire axis by the strong electric field during ONP.[8] After F4-TCNQ doping, these chains aggregate as a result of strong electrostatic interaction between F4-TCNQ molecules and P3HT chains. The P3HT chains with random orientation in NWs before annealing can be more directional along the wire axis after annealing because of thermal movement of P3HT chains and the rigidity of the F4-TCNQ molecular structure, resulting in enhanced charge transport. However, this synergistic effect of doping and thermal annealing is only possible at small amount of F4-

DOI: 10.1021/acsami.5b05647
ACS Appl. Mater. Interfaces 2015, 7, 18909−18914

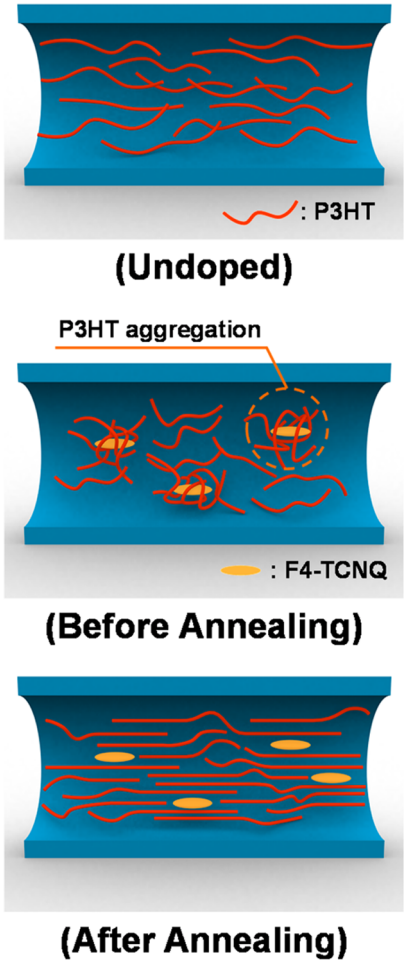

Figure 5. Schematic illustration of the microstructure change of P3HT chain in NW with thermal annealing: undoped NW before annealing (top), and doped NW before (center) and after (bottom) annealing.

TCNQ doping (0.5−1 wt %). When the doping ratio of F4-TCNQ exceeds 2.5 wt %, the high number of charge-transfer complexes between F4-TCNQ molecules and P3HT cause an increment of the rigidity of the P3HT backbone, which hinders the thermal movement of the P3HT chains and degrades the device electrical characteristics.[23,25]

In conclusion, we demonstrated the highly aligned P3HT NW FETs doped with F4-TCNQ molecules using practical NW printing technique, ONP, and investigated the synergistic effect of doping and thermal annealing on P3HT NWs. Thermal annealing activates the effect of molecular doping, and the device characteristics improved as the annealing temperature increased. After annealing at 200 °C, the P3HT NW FET doped with 1 wt % F4-TCNQ showed μ_{FET} of ~1×10^{-3} cm^2 V^{-1} s^{-1}, which was an order of magnitude higher than those of undoped or unannealed NW devices (~1×10^{-4} cm^2 V^{-1} s^{-1}). The activation of the doping effect by thermal annealing is correlated with the microstructure of the P3HT chain. F4-TCNQ molecules induce the aggregation of P3HT chains after doping due to strong electrostatic interaction between P3HT chain and F4-TCNQ molecules. The P3HT chains in NWs with random orientation before annealing can be more aligned along the wire axis by the thermal movement of P3HT chains after annealing, thereby resulting in improved charge transport in the NWs. These results can provide a promising strategy to apply highly integrated OSNWs to practical nanoelectronic applications.

■ ASSOCIATED CONTENT

Supporting Information

The Supporting Information is available free of charge on the ACS Publications website at DOI: 10.1021/acsami.5b05647.

Experimental procedures, output characteristics of the devices, TEM and elemental analysis results of P3HT NW, PL decay curves of doped NWs, threshold voltages of the devices (PDF)

■ AUTHOR INFORMATION

Corresponding Author

*E-mail: twlee@postech.ac.kr or taewlees@gmail.com.

Notes

The authors declare no competing financial interest.

■ ACKNOWLEDGMENTS

This work was supported by the Center for Advanced Soft-Electronics funded by the Ministry of Science, ICT and Future Planning as Global Frontier Project (2014M3A6A5060947). This research was also supported by Basic Science Research Program through the National Research Foundation of Korea (NRF) by the Ministry of Science, ICT & Future Planning (NRF-2013R1A1A2012660).

■ ABBREVIATIONS

P3HT, poly(3-hexylthiophene)
NW, nanowire
F4-TCNQ, 2,3,5,6-tetrafluoro-7,7,8,8-tetracyanoquinodimethane
OSNW, organic semiconducting nanowire
ONP, electrohydrodynamic organic nanowire printing
FET, field-effect transistor
HOMO, highest occupied molecular orbital
μ_{FET}, field-effect mobility
PEO, poly(ethylene oxide)
PL, photoluminescence

■ REFERENCES

(1) Briseno, A. L.; Mannsfeld, S. C. B.; Jenekhe, S. A.; Bao, Z.; Xia, Y. Introducing Organic Nanowire Transistors. *Mater. Today* **2008**, *11*, 38−47.
(2) Vohra, V.; Giovanella, U.; Tubino, R.; Murata, H.; Botta, C. Electroluminescence from Conjugated Polymer Electrospun Nanofibers in Solution Processable Organic Light-Emitting Diodes. *ACS Nano* **2011**, *5*, 5572−5578.
(3) Yang, H.; Lightner, C. R.; Dong, L. Light-Emitting Coaxial Nanofibers. *ACS Nano* **2012**, *6*, 622−628.
(4) Fang, J.; Wang, X.; Lin, T. Electrical Power Generator from Randomly Oriented Electrospun Poly(Vinylidene Fluoride) Nanofibre Membranes. *J. Mater. Chem.* **2011**, *21*, 11088−11091.
(5) Kim, I.-D.; Rothschild, A.; Lee, B. H.; Kim, D. Y.; Jo, S. M.; Tuller, H. L. Ultrasensitive Chemiresistors Based on Electrospun TiO_2 Nanofibers. *Nano Lett.* **2006**, *6*, 2009−2013.
(6) Cho, H.; Min, S.-Y.; Lee, T.-W. Electrospun Organic Nanofiber Electronics and Photonics. *Macromol. Mater. Eng.* **2013**, *298*, 475−486.
(7) Min, S.-Y.; Kim, T.-S.; Lee, Y.; Cho, H.; Xu, W.; Lee, T.-W. Organic Nanowire Fabrication and Device Applications. *Small* **2015**, *11*, 45−62.
(8) Min, S.-Y.; Kim, T.-S.; Kim, B. J.; Cho, H.; Noh, Y.-Y.; Yang, H.; Cho, J. H.; Lee, T.-W. Large-Scale Organic Nanowire Lithography and Electronics. *Nat. Commun.* **2013**, *4*, 1773.

DOI: 10.1021/acsami.5b05647
ACS Appl. Mater. Interfaces 2015, 7, 18909−18914

(9) Hwang, S. K.; Min, S.-Y.; Bae, I.; Cho, S. M.; Kim, K. L.; Lee, T.-W.; Park, C. Non-Volatile Ferroelectric Memory with Position-Addressable Polymer Semiconducting Nanowire. *Small* **2014**, *10*, 1976−1984.
(10) Lee, Y.; Kim, T.-S.; Min, S.-Y.; Xu, W.; Jeong, S.-H.; Seo, H.-K.; Lee, T.-W. Individually Position-Addressable Metal-Nanofiber Electrodes for Large-Area Electronics. *Adv. Mater.* **2014**, *26*, 8010−8016.
(11) Xu, W.; Seo, H.-K.; Min, S.-Y.; Cho, H.; Lim, T.-S.; Oh, C.; Lee, Y.; Lee, T.-W. Rapid Fabrication of Designable Large-Scale Aligned Graphene Nanoribbons by Electro-Hydrodynamic Nanowire Lithography. *Adv. Mater.* **2014**, *26*, 3459−3464.
(12) Xu, W.; Lim, T.-S.; Seo, H.-K.; Min, S.-Y.; Cho, H.; Park, M.-H.; Kim, Y.-H.; Lee, T.-W. N-Doped Graphene Field-Effect Transistors with Enhanced Electron Mobility and Air-Stability. *Small* **2014**, *10*, 1999−2005.
(13) Kim, G.; Kang, S.-J.; Dutta, G. K.; Han, Y.-K.; Shin, T. J.; Noh, Y.-Y.; Yang, C. A Thienoisoindigo-Naphthalene Polymer with Ultrahigh Mobility of 14.4 $cm^2/V{\cdot}s$ That Substantially Exceeds Benchmark Values for Amorphous Silicon Semiconductors. *J. Am. Chem. Soc.* **2014**, *136*, 9477−9483.
(14) Niimi, K.; Kang, M. J.; Miyazaki, E.; Osaka, I.; Takimiya, K. General Synthesis of Dinaphtho[2,3-b:2′,3′-f]thieno[3,2-B]thiophene (DNTT) Derivatives. *Org. Lett.* **2011**, *13*, 3430−3433.
(15) Kang, M. J.; Doi, I.; Mori, H.; Miyazaki, E.; Takimiya, K.; Ikeda, M.; Kuwabara, H. Alkylated Dinaphtho[2,3-b:2′,3′-f]Thieno[3,2-b]Thiophenes (Cn-DNTTs): Organic Semiconductors for High-Performance Thin-Film Transistors. *Adv. Mater.* **2011**, *23*, 1222−1225.
(16) Yuan, Y.; Giri, G.; Ayzner, A. L.; Zoombelt, A. P.; Mannsfeld, S. C. B.; Chen, J.; Nordlund, D.; Toney, M. F.; Huang, J.; Bao, Z. Ultra-High Mobility Transparent Organic Thin Film Transistors Grown by an off-Centre Spin-Coating Method. *Nat. Commun.* **2014**, *5*, 3005.
(17) Shtein, M.; Mapel, J.; Benziger, J. B.; Forrest, S. R. Effects of Film Morphology and Gate Dielectric Surface Preparation on the Electrical Characteristics of Organic-Vapor-Phase-Deposited Pentacene Thin-Film Transistors. *Appl. Phys. Lett.* **2002**, *81*, 268−270.
(18) Kobayashi, S.; Nishikawa, T.; Takenobu, T.; Mori, S.; Shimoda, T.; Mitani, T.; Shimotani, H.; Yoshimoto, N.; Ogawa, S.; Iwasa, Y. Control of Carrier Density by Self-Assembled Monolayers in Organic Field-Effect Transistors. *Nat. Mater.* **2004**, *3*, 317−322.
(19) Cho, S.; Lee, K.; Yuen, J.; Wang, G.; Moses, D.; Heeger, A. J.; Surin, M.; Lazzaroni, R. Thermal Annealing-Induced Enhancement of the Field-Effect Mobility of Regioregular Poly(3-Hexylthiophene) Films. *J. Appl. Phys.* **2006**, *100*, 114503.
(20) Abe, Y.; Hasegawa, T.; Takahashi, Y.; Yamada, T.; Tokura, Y. Control of Threshold Voltage in Pentacene Thin-Film Transistors Using Carrier Doping at the Charge-Transfer Interface with Organic Acceptors. *Appl. Phys. Lett.* **2005**, *87*, 153506.
(21) Gao, W.; Kahn, A. Controlled *p*-Doping of Zinc Phthalocyanine by Coevaporation with Tetrafluorotetracyanoquinodimethane: A Direct and Inverse Photoemission Study. *Appl. Phys. Lett.* **2001**, *79*, 4040−4042.
(22) Yim, K.-H.; Whiting, G. L.; Murphy, C. E.; Halls, J. J. M.; Burroughes, J. H.; Friend, R. H.; Kim, J.-S. Controlling Electrical Properties of Conjugated Polymers via a Solution-Based p-Type Doping. *Adv. Mater.* **2008**, *20*, 3319−3324.
(23) Ma, L.; Lee, W. H.; Park, Y. D.; Kim, J. S.; Lee, H. S.; Cho, K. High Performance Polythiophene Thin-Film Transistors Doped with Very Small Amounts of an Electron Acceptor. *Appl. Phys. Lett.* **2008**, *92*, 063310.
(24) Wei, P.; Oh, J. H.; Dong, G.; Bao, Z. Use of a 1H-Benzoimidazole Derivative as an *n*-Type Dopant and to Enable Air-Stable Solution-Processed *n*-Channel Organic Thin-Film Transistors. *J. Am. Chem. Soc.* **2010**, *132*, 8852−8853.
(25) Ma, L. Effect of Annealing on Microstructure and Electrical Characteristics of Doped Poly (3-Hexylthiophene) Films. *Chin. Phys. Lett.* **2010**, *27*, 128502.
(26) Pingel, P.; Neher, D. Comprehensive Picture of *p*-Type Doping of P3HT with the Molecular Acceptor F_4TCNQ. *Phys. Rev. B: Condens. Matter Mater. Phys.* **2013**, *87*, 115209.
(27) Gao, J.; Roehling, J. D.; Li, Y.; Guo, H.; Moulé, A. J.; Grey, J. K. The Effect of 2,3,5,6-Tetrafluoro-7,7,8,8-Tetracyanoquinodimethane Charge Transfer Dopants on the Conformation and Aggregation of Poly(3-Hexylthiophene). *J. Mater. Chem. C* **2013**, *1*, 5638−5646.
(28) Horowitz, G.; Delannoy, P. An Analytical Model for Organic-Based Thin-Film Transistors. *J. Appl. Phys.* **1991**, *70*, 469−475.
(29) Lakowicz, J. R. *Principles of Fluorescence Spectroscopy*, 3rd ed.; Springer: Berlin, 2006.
(30) Shi, Y.; Liu, J.; Yang, Y. Device Performance and Polymer Morphology in Polymer Light Emitting Diodes: The Control of Thin Film Morphology and Device Quantum Efficiency. *J. Appl. Phys.* **2000**, *87*, 4254−4263.

DOI: 10.1021/acsami.5b05647
ACS Appl. Mater. Interfaces 2015, 7, 18909−18914